variety of tumors in animal models [16-19]. The anti-tumor activity of IL-12 is considered to be due to anti-angiogenic effects as well as to induction of immune response [19-21]. The number of $CD8^+$ T cells and dendritic cells is significantly elevated in induced murine mammary tumors stably transfected with VEGF-C siRNA, suggesting that VEGF-C modulates the immune response [22]. Based on the above evidence, we chose to use an immunocompetent mammary cancer model in this study.

2. Materials and methods

2.1 BJMC3879 cell line

Mouse mammary tumor virus (MMTV), isolated and purified from medium in which Jyg-MC cells (established from mammary tumors of the Chinese wild mouse) were grown, was inoculated into the inguinal mammary glands of female BALB/c mice, resulting in the development of mammary carcinomas [23]. The BJMC3879 mammary adenocarcinoma cell line was subsequently derived from a metastatic focus within a lymph node from one of the inoculated mice and the cell line continues to show a high metastatic propensity, especially to lymph nodes and lungs [19,24,25]. We maintain the BJMC3879 cell line in either RPMI-1640 medium or Dulbecco's Modified Eagle's medium containing 10% fetal bovine serum supplemented with streptomycin/penicillin in an incubator at 37°C under a 5% CO_2 atmosphere.

2.2 Animals

Forty female 6-week-old BALB/c mice were used in this study (Japan SLC, Inc., Hamamatsu, Japan). The animals were housed no more than 5 per plastic cage on wood chip bedding with free access to water and food and maintained under conditions of controlled temperature (21 ± 2 °C), humidity (50 ± 10 %), and lighting (12 h-12 h light-dark cycle). All animals were held for a 1-week acclimatization period before study commencement. This animal experiment was approved by the Animal Experiment Committee of Osaka Medical College. Husbandry was in accordance with the procedures outlined in the Guide for the Care and Use of Laboratory Animals at Osaka Medical College, the Japanese Government Animal Protection and Management Law (No.105) and the Japanese Government Notification on Feeding and Safekeeping of Animals (No.6).

2.3 Vectors for VEGF-C siRNA and IL-12 expression

We used short hairpin RNAs (shRNA) targeting mouse VEGF-C to generate siRNA. The previously determined mouse VEGF-C siRNA sequence, 5'-GCATGAACACCAGCACAGGTT*ccaagag*AACCTGTGCTGGTGTTCATGC-3', [13] contains a 21-nucleotide sequence in sense and antisense orientation separated by a 7-nucleotide spacer (indicated above by small letters in italics). The complementary oligonucleotide was annealed and ligated into a *Bbs*I/*Bbs*I-digested psiRNA-h7SKGFP-zeo vector (InvivoGen, Inc., San Diego, CA, USA). This vector contains the human 7SK promoter (an RNA polymerase III promoter), which can generate high amounts of shRNAs [26]. We identified positive clones by restriction digestion and confirmed by sequencing.

The plasmid, pORF-mIL-12 (InvivoGen, Inc., San Diego, CA, USA), encodes for the mouse IL-12 gene; it is an active fusion of the p35 and p40 subunits linked by bovine elastin motifs to express IL-12 as a single peptide with the signal sequence in the p35 subunit. This vector

is regulated by the elongation factor -1α (EF-1α)/human T cell leukemia virus type 1 (HTLV-1) long terminal repeat hybrid promoter and has previously shown anti-neoplastic effects [19]. To produce the empty control vector, we deleted the *IL-12* gene from pORF-mIL-12 via digestion with *NcoI/NheI*.

2.4 *In vivo* gene therapy using VEGF-C siRNA and/or IL12 expression vectors

BJMC3879 cells (5 x 10^6 cells/0.3 ml in phosphate buffered saline) were inoculated into the right inguinal region of the 40 female BALB/c mice and the animals randomly allocated into 4 groups - pVec (control), psiVEGF-C, pIL12, and psiVEGF-C+pIL12 - of 10 mice each. Two weeks post-inoculation, when the tumors had reached 0.2–0.4 cm in diameter, we injected either psiVEGF-C, pIL12 or psiRNA-VEGF-C+pIL12, or the pVec control directly into the tumors of mice in the appropriate treatment groups. The vectors were injected using a 27-guage needle at a concentration of 0.5μg/μl in sterile saline while the animals were under isoflurane anesthesia. A total volume of 150 μl was introduced into larger tumors (more than 0.6 cm in maximum diameter), while smaller tumors of 0.6 cm in maximum diameter were infused until we detected leakage of the vector solution. Immediately after vector injection, we performed *in vivo* gene electrotransfer by applying a conductive gel (Echo Jelly; Aloka., Co., Ltd., Tokyo, Japan) topically to the unshaved skin over the injected tumor. Electric pulses were delivered directly to the tumor via "forceps" platinum plate electrodes (CUY650-10; Nepa Gene Co., Ltd., Ichikawa, Japan) using a CUY21EDIT square-wave electropulser (Nepa Gene Co., Ltd.). We had previously determined the parameters for optimal gene electrotransfer: for intratumoral injection of 50-75 μg plasmid (dependent on tumor size as mentioned above), 8 pulses with a pulse length of 20 milliseconds at 100 volts proved to be most efficient [13,24,27].

Using calipers, we measured the size of each treated mammary tumor weekly and calculated tumor volumes using the formula *maximum diameter x (minimum diameter)*^{2} *x 0.4* [28]. Individual body weights were also recorded at weekly intervals. All surviving animals received 50 mg/kg 5-bromo-2'-deoxyuridine (BrdU; Sigma Co., St. Lois, MO, USA) i.p. at 1 h prior to sacrifice.

2.5 Histopathological analysis

After 8 weeks of treatment and observation/ tumor measurement, all mice were euthanized under isoflurane anesthesia and the mammary tumors and certain lymph nodes (specifically, nodes from axillary and femoral regions, as well as any that appeared abnormal) were removed. We then immediately fixed a portion of each tissue sample in 10% phosphate-buffered formalin. Lungs were routinely inflated with the fixative, excised, and immersed back into the phosphate-buffered formalin. We subsequently trimmed and examined all lobes for metastatic foci before processing all tissues through to paraffin blocks, after which they were cut into 4-μm-thick sections and stained with hematoxylin and eosin (H&E) for histopathological examination or left unstained for immunohistochemistry.

2.6 Immunohistochemical analysis of mammary tumors for microvascular density and dilated lymphatic vessels

To quantitatively assess blood and lymphatic microvessel density in the primary mammary carcinomas, we used the avidin-biotin immunohistochemical complex method (LSAB kit;

DakoCytomation) with a rabbit polyclonal antibody against CD31 (Lab Vision Co., CA, USA), a specific marker for blood vessel endothelium, and a hamster anti-podoplanin monoclonal antibody (AngioBio Co., Del Mar, CA, USA) targeted to lymphatic endothelium. The number of CD31-positive blood microvessels was counted as previously described [29]; briefly, we scanned slides at low-power (X100) magnification to identify those areas having the highest number of vessels and the 5 areas of highest microvascular density were then selected and counted at higher (X200–400) magnification to obtain mean ± SD values. We counted the number of podoplanin-positive lymphatic vessels containing intralumenal tumor cells and expressed the numbers of immunopositive structures as an average ± SD.

2.7 Statistical analyses

We analyzed significant differences in the quantitative data between groups using the Student's *t*-test via the method of Welch, which provides for insufficient homogeneity of variance. The differences in metastatic incidence we examined by Fisher's exact probability test, with $P<0.05$ or $P<0.01$ considered to represent a statistically significant difference.

3. Results

3.1 Body weights and tumor growth

No mortality was observed in this study. At experimental weeks 2 through 6, body weights in mice receiving pIL12 and the combination psiVEGF-C + pIL12 treatment began to decrease compared to both control and psiVEGF-C alone. Though mild (less than 5% reduction compared to the controls), weight loss was consistently significant in the combination group during this 4-week period, but the pIL12 group showed statistically lower weights intermittently at weeks 2 and 4 (Fig. 1A). The general condition of the animals was good throughout the experiment. At conclusion of the study at week 8, body weights were roughly equivalent across treatment groups; however, as can be seen in Figure 1B, the tumor volumes of all 3 treatment groups were significantly suppressed from experimental weeks 3 to termination as compared to the pVec controls. The average tumor volumes at week 8 were as follows: pVec control group, 1715 ± 662 mm^3; psiVEGF-C group, 954 ± 470 mm^3; pIL12 group, 756 ± 343 mm^3; psiVEGF-C + pIL12 group, 860 ± 437 mm^3.

3.2 Tumor morphology and metastases

Histopathologically, all mammary carcinomas proved to be moderately differentiated adenocarcinomas. Representative histologic morphologies of lymph node and lung metastases are illustrated in Figures 2A-H. Both the metastatic incidence and multiplicity in lymph node and lung was markedly reduced in all treatment groups as compared to control; as illustrated in Figures 3A and B for lymph node metastasis and Figures 3C and D for lung metastasis, the reductions were statistically significant within the parameters of overall node and lung metastatic incidence and in the number of larger metastatic lung foci >250 μm. Treatment with pIL12 alone appears to be more effective in inhibiting tumor spread than psiVEGF-C, but by all criteria evaluated, the psiVEGF-C + pIL12 combination yielded the greatest reductions in metastatic spread and severity over either psiVEGF-C alone, pIL12 alone, or pVec control (Figures.3B and D).

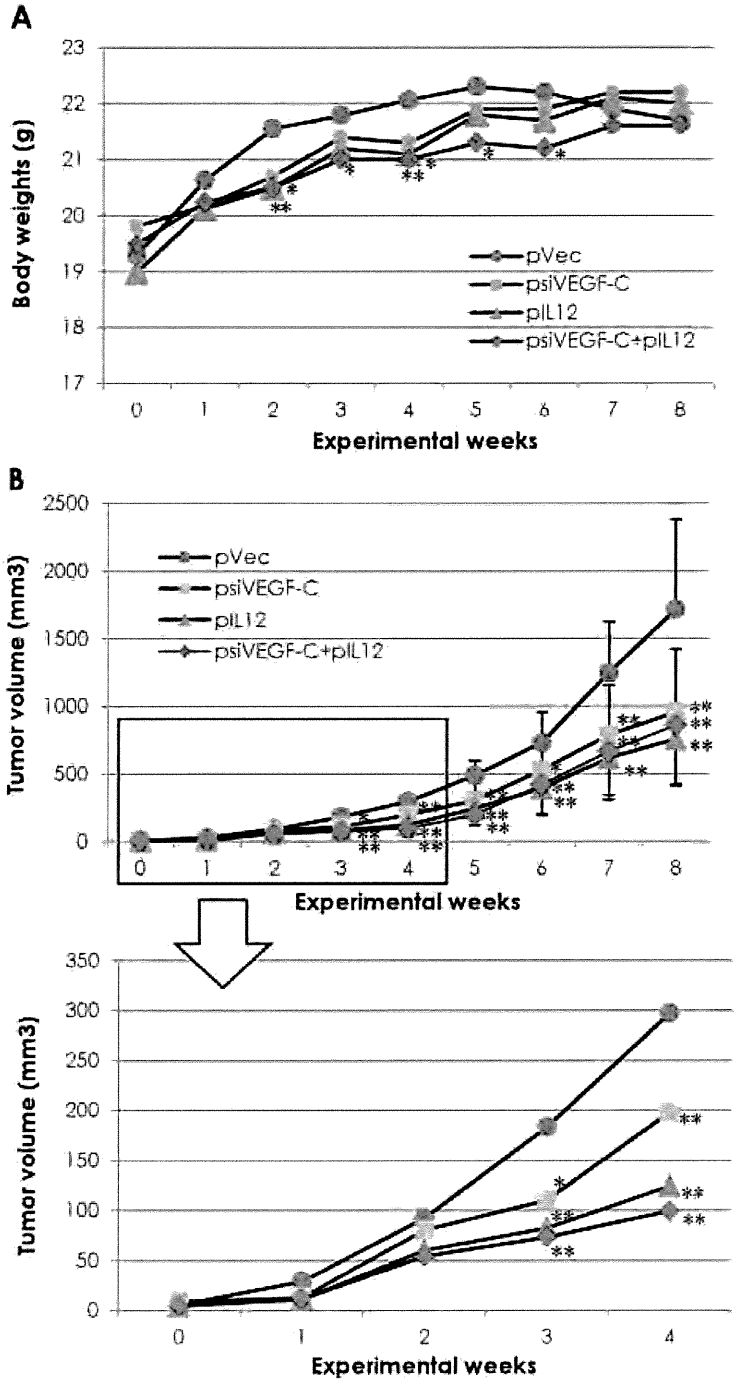

Fig. 1. Body weights (**A**) and mammary tumor volumes (**B**) in female BALB/c mice treated with pVec (control), psiVEGF-C, pIL12, and the psiVEGF-C+pIL12 combination vector. (**A**) Body weights were significantly lower in the pIL12 group at weeks 2 and 4, and in the psiVEGF-C+pIL12 combination group from weeks 2 through 6, as compared to the pVec group. (**B**) Increases in tumor volume were significantly suppressed in mice transfected with either psiVEGF-C alone, pIL12 alone, or combined psiVEGF-C+pIL12 at weeks 3 – 8 (experiment termination) compared to pVec -treated control mice. The data for body weights at weeks 0 – 4 are magnified. Data represent mean ± SD. **P*<0.05; ***P*<0.01 compared with pVec controls.

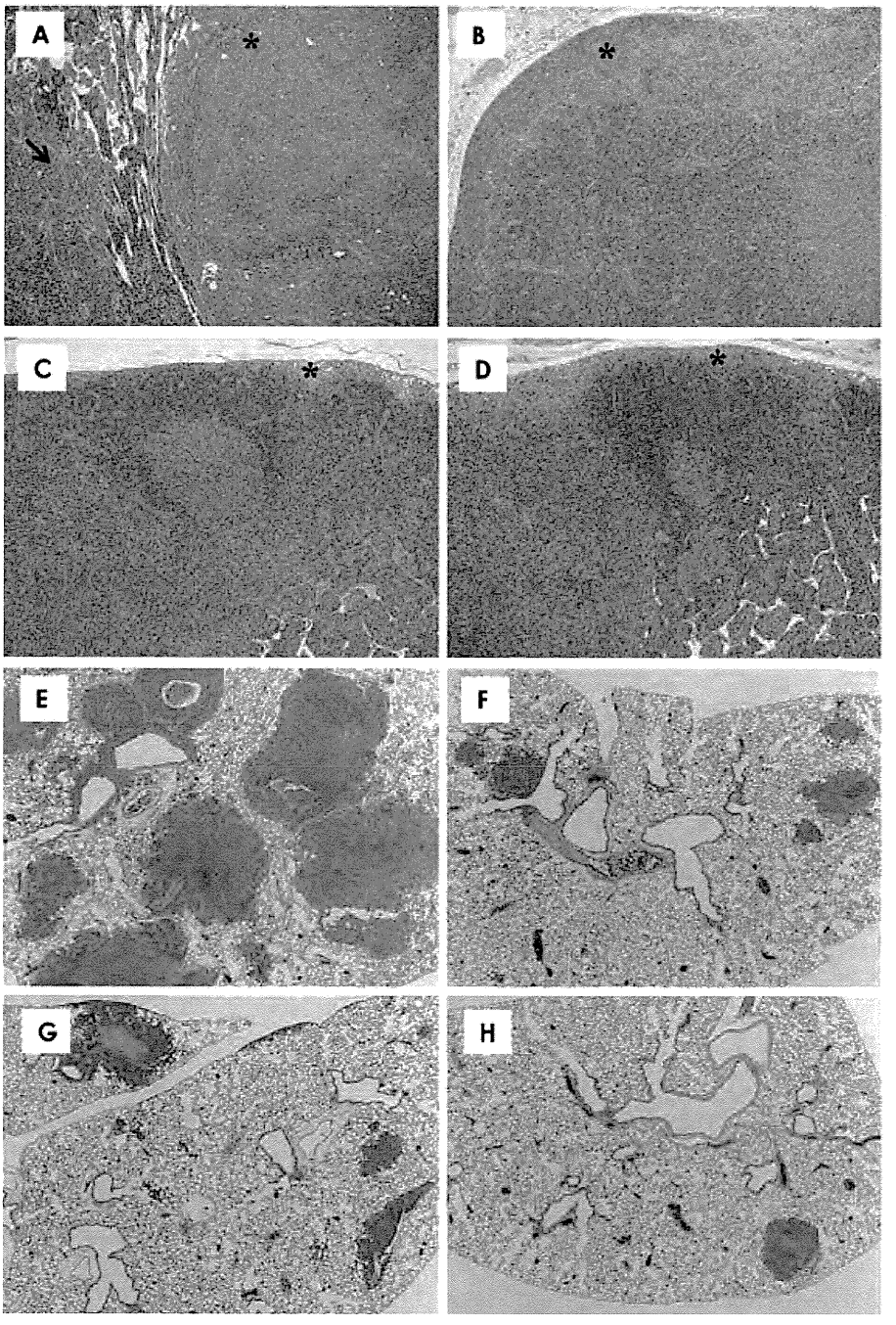

Fig. 2. Metastasis to a lymph node (**A-D**). (**A**) Metastatic carcinoma cells fill the sinusoidal space (arrow) in a control mouse. (**B**) A lymph node from a tumor injected with psiVEGF-C. Metastatic carcinoma cells filled the subcapsular sinus (asterisk). (**C**) and (**D**) No metastatic cells are observed in the subcaspsular sinus of a lymph node from a mouse in the pIL12 group (**C**), or from an animal in the combination psiVEGF-C+pIL12 group (**D**), but histiocytes are acummulating here in each case (asterisks). (**E**) Metastatic foci in the lung of a control (pVec) mouse. Many metastatic foci and small to large nodules were seen. (**F-H**) Metastatic foci tended to be smaller in mice receiving psiVEGF-C (**F**), pIL12 (**G**), and the combination vector (**H**) than those observed in the pVec group (**E**). H&E staining. Magnification: **A-D**, x100; **E-H**, x40.

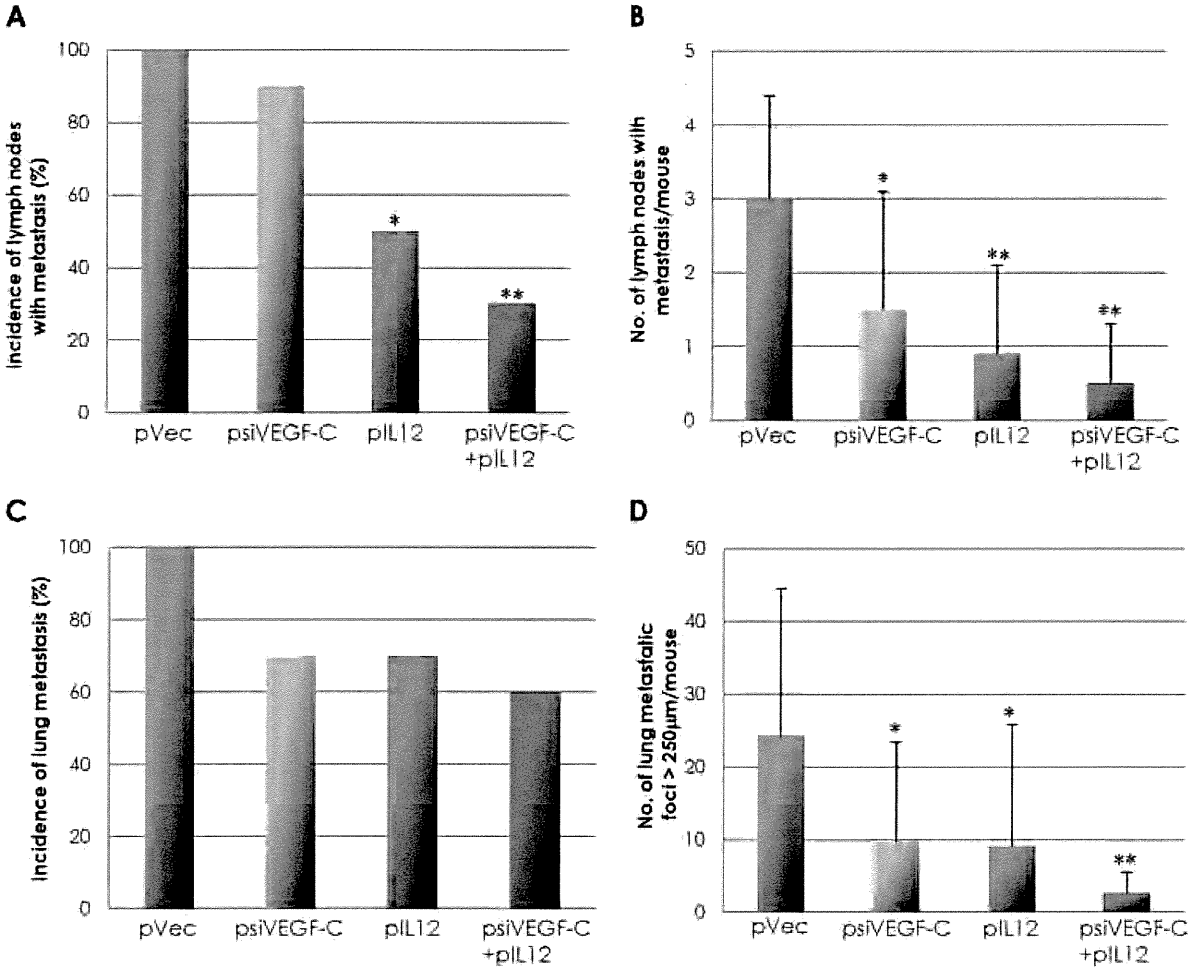

Fig. 3. Quantitative analysis of lymph node metastasis (**A** and **B**) and lung metastasis (**C** and **D**) in mice treated with pVec (control), psiVEGF-C alone, pIL12 alone, or combined psiVEGF-C+pIL12. (**A**) The incidence of lymph node metastasis was 100% in the pVec group, while the incidence was 90% in the psiVEGF-C group, 50% in the pIL12 group and 30% in the psiVEGF-C+pIL12 group; these incidences were significantly lower with pIL12 alone and pIL12 combine with psiVEGF-C. (**B**) Similarly, the number of lymph nodes with metastases per mouse was also significantly decreased in all groups receiving therapeutic treatment. (**C**) The incidence of lung metastasis tended to decrease in all therapeutic groups, but the decrease was not statistically significant. (**D**) However, the number of lung metastatic nodules >250 μm was significantly lower in all groups receiving therapeutic treatment. Data represent mean ± SD. **P*<0.05; ***P*<0.01

3.3 Angiogenesis as measured by microvessel density

The immunohistochemical appearance of microvessels immunopositive for CD31, which is specific for the endothelium of blood vessels, is represented in Figures 4A and B. Tumor angiogenesis, as determined by the number of stained microvessels within the tumors themselves, was significantly lower in all therapeutic groups when compared to the pVec control group (Figure 5A).

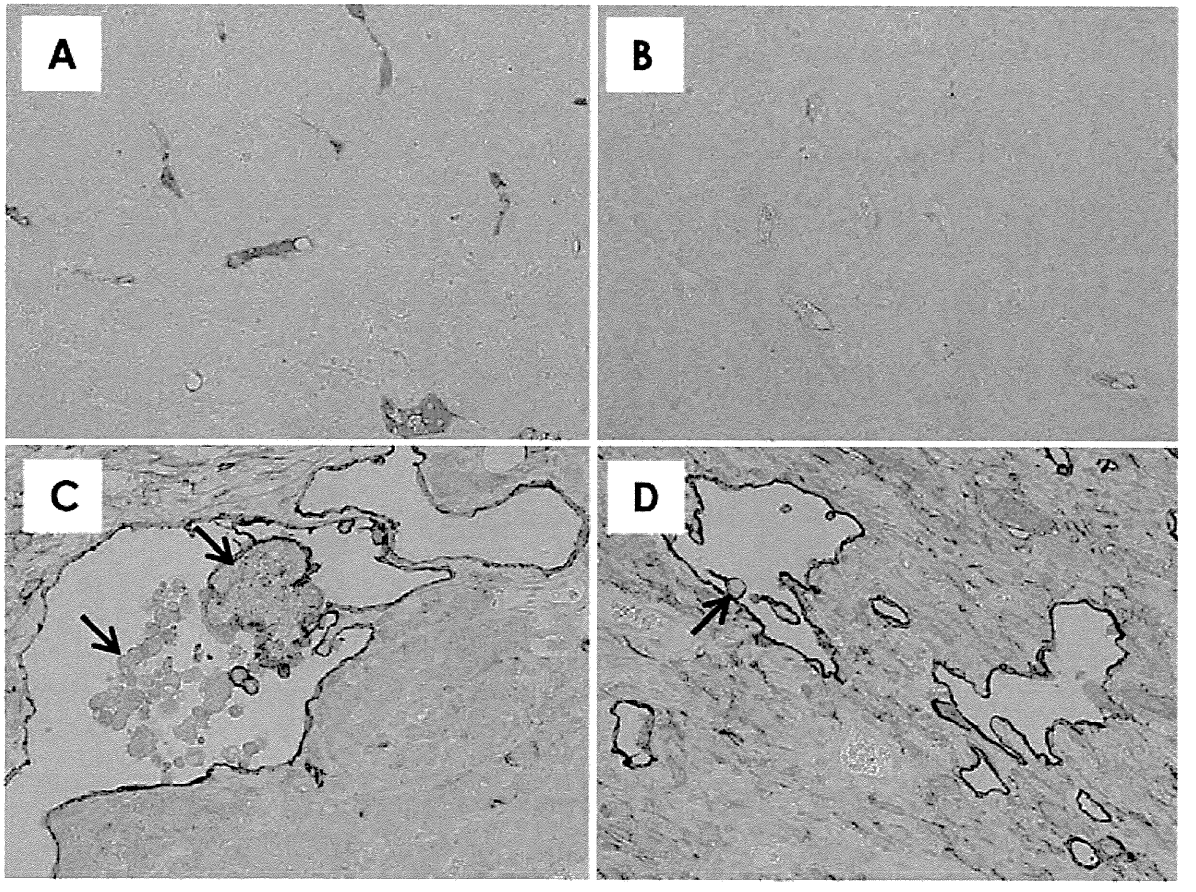

Fig. 4. Immunohistochemical analysis of angiogenesis (**A** and **B**) and lymphangiogenesis (**C** and **D**) in mammary tumors transfected with pVec (control), psiVEGF-C alone, pIL12 alone, or combined psiVEGF-C+pIL12. (**A**) A section representative of control tumors show a higher density of well-developed CD31-positive microvessels, whereas in tumors transfected with psiVEGF-C alone, pIL12 alone, or combined psiVEGF-C+pIL12 (**B**), few immunopositive vessels are seen. (**C**) Lymphatic vessels were often dilated and frequently contained migrating tumor cells within the lumina (arrows, pVec-transfected tumor). (**D**) The numbers of lymphatic vessels containing intralumenal tumor cells were lower in tumors transfected with psiVEGF-C alone, pIL12 alone, or combined psiVEGF-C+pIL12 (arrow). **A** and **B**, anti-CD31 immunohistochemistry; **C** and **D**, anti-podoplanin immunohistochemistry. Magnification: **A-D**, x400.

3.4 Dilated lymphatic vessels

The relative decrease in the number of dilated lymphatic vessels containing intraluminal tumor cells indicates migratory inhibition of cancer cells via the lymphatics of the tumor. Anti-podoplanin staining of the lymphatic microvessels in mammary tumors is demonstrated in Figures 4C and D. In all groups, these lymphatic microvessels were well developed in the outer, superficial layers of the mammary tumors in a somewhat hexagonal network pattern. We frequently observed tumor cells within the lumina of dilated lymphatic vessels in tumors of both control (Figure 4C) and treated animals (Figure 4D). However, as shown in Figure 5B, the number of lymphatic vessels carrying detached cancer cells was lower in both the pIL12 and psiVEGF-C + pIL12 groups, but this difference was statistically

significant only in the mice receiving pIL12 alone. The data from mice treated with psiVEGF-C alone showed large variations.

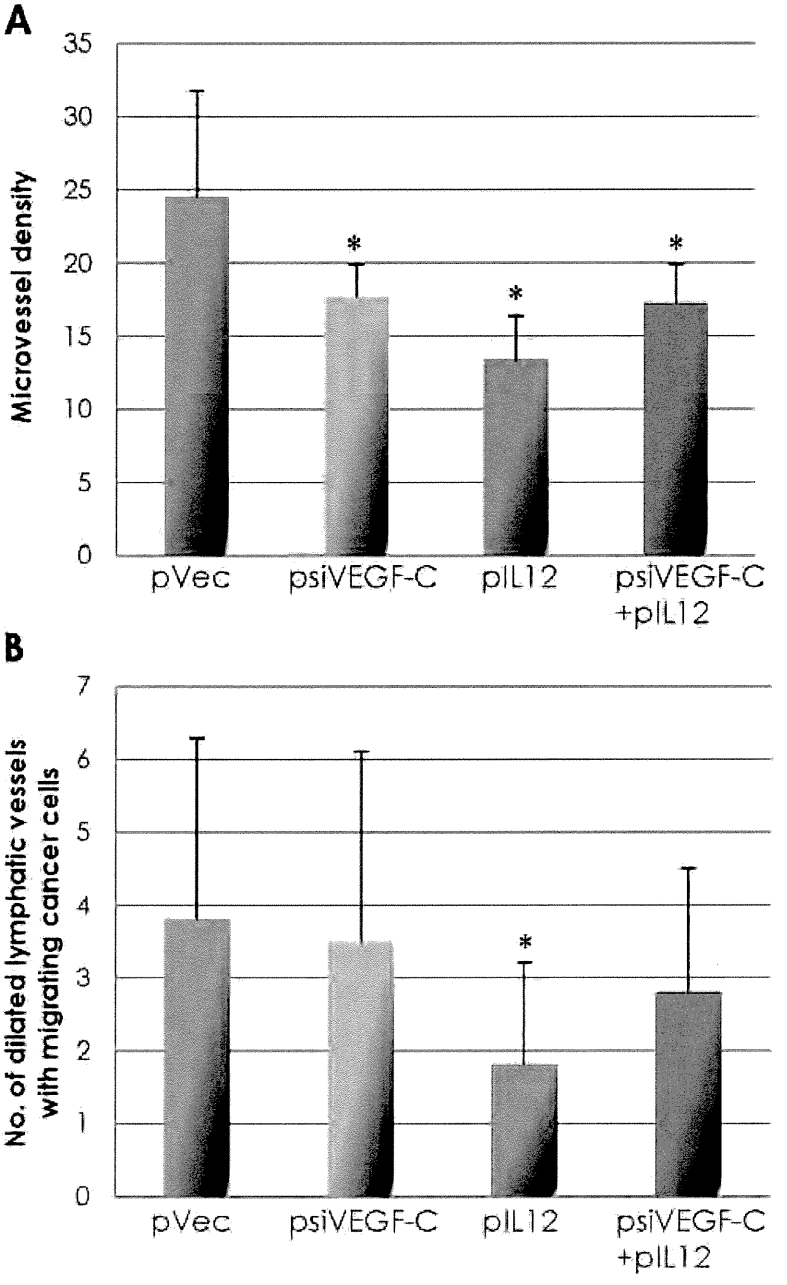

Fig. 5. Microvessel density (**A**) and frequency of lymphatic vessels containing migrating cancer cells (**B**) from tumors transfected with pVec (control), psiVEGF-C alone, pIL12 alone or combined psiVEGF-C+pIL12. (**A**) Microvessel density was significantly lower in tumors of mice receiving therapeutic vectors compared to the pVec control. (**B**) The number of lymphatic vessels containing intraluminal cancer cells was lower in the tumors transfected with pIL12 alone and combined psiVEGF-C+pIL12 as compared with the pVec controls, but significant differences were observed in the pIL12 alone group only. Data represent mean ± SD. *P<0.05.

4. Discussion

Since metastasis seems to be the biggest prognostic factor for lethality in most cancers, finding therapies that control or totally inhibit tumor spread is of paramount importance. A variety of mechanisms may contribute to the dissemination of primary cancer cells: local tissue invasion, systemic metastasis via tumor blood vessels to distant organs, and lymphatic metastasis via tumor lymphatic vessels to the sentinel lymph node, distal lymph nodes, and from there to distal organs. In general, the most common pathway of initial dissemination is via the lymphatics, with patterns of spread via afferent ducts [30]. The lymphatic capillaries present in tissues and tumors provide entrance into the lymphatic system, allowing cancer cell migration to the lymph nodes. In this study, lymph node metastasis was significantly decreased by exposure to vectors expressing siVEGF-C, IL-12, or a combination vector expressing both. We also observed a significant decrease in the number of lymphatic vessels containing tumor cells intraluminally in tissues from mice receiving pIL12 alone and the combination of psiVEGF-C/pIL12, suggesting an inhibitory effect on migration into tumor lymphatic vessels that supports the significant reduction in lymph node metastasis in these groups.

VEGF-C expression has been shown to correlate with lymph node metastasis in a variety of human cancers, including breast [6,31]. In many animal models of cancer, VEGF-C has been shown to enhance tumor lymphangiogenesis, the metastatic spread of tumor cells to lymph nodes and, in some cases, to distant organs [32]. Downregulation of VEGF-C using siRNA has been shown to reduce lymph node and lung metastases in murine mammary cancer models [13,22]. In 2009, an endogenous soluble isoform of VEGFR-2 (sVEGFR-2) that sequesters VEGF-C was identified and shown to be the first endogenous specific inhibitor of lymphatic vessel growth [33]. Endogenous sVEGFR-2 is a truncated form of 230 kDa membrance-bound form of VEGFR-2 resulting from alternative splicing. Subsequently, it has been shown that endogenous sVEGFR-2 suppresses tumor growth and lymph node metastasis in a mouse mammary cancer model [34]. This molecule significantly inhibits lymphangiogenesis, but not angiogenesis, in mammary tumor tissues [34]. In addition, VEGFR-3, the VEGF-C receptor, is predominantly expressed on lymphatic endothelial cells [35], and VEGF-C-dependent activation of VEGFR-3 stimulates the growth of lymph endothelial cells and lymphatics [36]. Blockade of VEGFR-3 signaling by soluble VEGFR-3 inhibits lymphangiogenesis and lymph node metastasis in experimental animal cancer models [11,37,38].

Cancer cells metastasize to distal sites via the vascular system as well as via the lymphatic system. Significant decreases in microvessel density were observed in the tumors we injected with psiVEGF-C, pIL12, and the combination vector. VEGF-C has been reported to stimulate angiogenesis under certain experimental conditions [39]. The biosynthesis of VEGF-C involves proteolytic processing that gives intermediate forms along with a 21kDa mature form [36]. The intermediate forms predominantly bind to VEGFR-3, whereas the mature form can bind to both VEGFR-3 and VEGFR-2 to induce angiogenesis [36], which explains the inhibition of angiogenesis observed with exposure to psiVEGF-C [36,40]and which is in agreement with our previous VEGF-C siRNA experiment [13].

In contrast, IL-12 has also been shown to strongly inhibit angiogenesis in mouse corneal neovascularization [20] and in several tumor models [19,21]. IL-12 itself has no direct action on vascular endothelial cells; however, IL-12 induction of IFNγ can apparently suppress angiogenesis on Matrigel-cultured human umbilical vein endothelial cells [19]. But IFNγ

does not seem the only player in angiogenesis inhibition; the cytokine IP-10 (IFNγ-inducing protein-10) has also been reported to be a potent antiangiogenic factor *in vivo* [41]. The exact mechanism of angiogenic suppression induced by IL-12 is therefore another avenue to explore in tumor therapeutics.

And the means of administration may also affect the efficacy of IL-12 as an anti-angiogenic/anti-metastatic agent. In a phase I clinical trial, recombinant IL-12 stimulated significant immunological activity in cancer patients [42]. However, despite initial enthusiasm for recombinant IL-12 as a potential anti-tumor agent, severe systemic toxicities have repeatedly been reported in clinical trials, limiting its use [43,44]. In contrast to direct cytokine administration, *IL-12* gene therapy using an adenoviral vector in animal cancer models has been shown to be as effective as protein exposure, but avoids the systemic toxicity seen in human trials [45-47]. One of the major advantages of gene transfer compared with the administration of recombinant proteins is the quicker achievement of steady-state levels of circulating protein [48]; administration of recombinant proteins leads first to a concentration peak, which may be within the zone of toxicity and responsible for adverse effects, followed by a rapid fall to sub-therapeutic levels.

The administration of either psiVEGF-C, pIL12, or a combination of both psiVEGF-C + pIL12 vectors significantly suppressed tumor growth and metastasis in our immunocompetent metastatic mammary cancer model. Since Carter *et al.* have reported the chance of tumor recurrence and/or metastasis increases dramatically once breast cancers reach 4 cm or larger [49], this reduction in tumor volume induced by decreasing VEGF-C and increasing IL-12 expression could be clinically significant; the fact that the treatment with a combined psiVEGF-C and pIL12 vector showed an enhanced inhibitory effect not only on tumor growth but also on metastasis is of particular importance when considering therapeutic strategies in breast cancer treatment. In conclusion, treatment with psiVEGF-C and pIL12 exerted combinational effects for suppression of tumor growth and metastasis in mouse mammary cancer model, suggesting a potentially significant clinical option in the treatment of metastatic human breast cancer.

5. Abbreviations

BrdU, 5-bromo-2'-deoxyuridine; *EF-1α/HTLV-1*, elongation factor -1α/human T cell leukemia virus type 1; *H&E*, hematoxylin and eosin; *IFNγ*, interferon-γ; *IL-12*, interleukin-12; *IP-10*, IFNγ-inducing protein-10; *MMTV*, mouse mammary tumor virus; *shRNA*, short hairpin RNAs; *siRNA*, short interfering RNA; *VEGF-C*, vascular endothelial growth factor-C; *VEGFR*, vascular endothelial growth factor receptor

6. Acknowledgements

This investigation was supported by a Grant-in-Aid for Scientific Research (C)(2) from the Ministry of Education, Culture, Sports, Science and Technology (MEXT) of Japan (No. 17591360 to M.A. Shibata).

7. References

[1] Guarneri, V., Conte, P.F. (2004), The curability of breast cancer and the treatment of advanced disease. *Eur J Nucl Med Mol Imaging* 31 Suppl 1, S149-61.

[2] Agarwal, G., Pradeep, P.V., Aggarwal, V., Yip, C.H., Cheung, P.S. (2007), Spectrum of breast cancer in Asian women. *World J Surg* 31, 1031-40.

[3] Brinton, L.A., Sherman, M.E., Carreon, J.D., Anderson, W.F. (2008), Recent trends in breast cancer among younger women in the United States. *J Natl Cancer Inst* 100, 1643-8.

[4] Bouchardy, C., Fioretta, G., Verkooijen, H.M., Vlastos, G., Schaefer, P., Delaloye, J.F., *et al.* (2007), Recent increase of breast cancer incidence among women under the age of forty. *Br J Cancer* 96, 1743-6.

[5] Nguyen, D.X., Massague, J. (2007), Genetic determinants of cancer metastasis. *Nat Rev Genet* 8, 341-52.

[6] Salven, P., Lymboussaki, A., Heikkila, P., Jaaskela-Saari, H., Enholm, B., Aase, K., *et al.* (1998), Vascular endothelial growth factors VEGF-B and VEGF-C are expressed in human tumors. *Am J Pathol* 153, 103-8.

[7] Mylona, E., Alexandrou, P., Mpakali, A., Giannopoulou, I., Liapis, G., Markaki, S., *et al.* (2007), Clinicopathological and prognostic significance of vascular endothelial growth factors (VEGF)-C and -D and VEGF receptor 3 in invasive breast carcinoma. *Eur J Surg Oncol* 33, 294-300.

[8] Nakamura, Y., Yasuoka, H., Tsujimoto, M., Imabun, S., Nakahara, M., Nakao, K., *et al.* (2005), Lymph vessel density correlates with nodal status, VEGF-C expression, and prognosis in breast cancer. *Breast Cancer Res Treat* 91, 125-32.

[9] Skobe, M., Hawighorst, T., Jackson, D.G., Prevo, R., Janes, L., Velasco, P., *et al.* (2001), Induction of tumor lymphangiogenesis by VEGF-C promotes breast cancer metastasis. *Nat Med* 7, 192-8.

[10] Karpanen, T., Egeblad, M., Karkkainen, M.J., Kubo, H., Yla-Herttuala, S., Jaattela, M., *et al.* (2001), Vascular endothelial growth factor C promotes tumor lymphangiogenesis and intralymphatic tumor growth. *Cancer Res* 61, 1786-90.

[11] He, Y., Kozaki, K., Karpanen, T., Koshikawa, K., Yla-Herttuala, S., Takahashi, T., *et al.* (2002), Suppression of tumor lymphangiogenesis and lymph node metastasis by blocking vascular endothelial growth factor receptor 3 signaling. *J Natl Cancer Inst* 94, 819-25.

[12] Mandriota, S.J., Jussila, L., Jeltsch, M., Compagni, A., Baetens, D., Prevo, R., *et al.* (2001), Vascular endothelial growth factor-C-mediated lymphangiogenesis promotes tumour metastasis. *EMBO J* 20, 672-82.

[13] Shibata, M.A., Morimoto, J., Shibata, E., Otsuki, Y. (2008), Combination therapy with short interfering RNA vectors against VEGF-C and VEGF-A suppresses lymph node and lung metastasis in a mouse immunocompetent mammary cancer model. *Cancer Gene Ther* 15, 776-786.

[14] Gubler, U., Chua, A.O., Schoenhaut, D.S., Dwyer, C.M., McComas, W., Motyka, R., *et al.* (1991), Coexpression of two distinct genes is required to generate secreted bioactive cytotoxic lymphocyte maturation factor. *Proc Natl Acad Sci U S A* 88, 4143-7.

[15] Colombo, M.P., Trinchieri, G. (2002), Interleukin-12 in anti-tumor immunity and immunotherapy. *Cytokine Growth Factor Rev* 13, 155-168.

[16] Coughlin, C.M., Wysocka, M., Trinchieri, G., Lee, W.M. (1997), The effect of interleukin 12 desensitization on the antitumor efficacy of recombinant interleukin 12. *Cancer Res* 57, 2460-7.

[17] Boggio, K., Nicoletti, G., Di Carlo, E., Cavallo, F., Landuzzi, L., Melani, C., *et al.* (1998), Interleukin 12-mediated prevention of spontaneous mammary adenocarcinomas in two lines of Her-2/neu transgenic mice. *J Exp Med* 188, 589-96.

[18] Roy, E.J., Gawlick, U., Orr, B.A., Rund, L.A., Webb, A.G., Kranz, D.M. (2000), IL-12 treatment of endogenously arising murine brain tumors. *J Immunol* 165, 7293-9.

[19] Shibata, M.A., Ito, Y., Morimoto, J., Kusakabe, K., Yoshinaka, R., Otsuki, Y. (2006), In vivo electrogene transfer of interleukin-12 inhibits tumor growth and lymph node and lung metastases in mouse mammary carcinomas. *J Gene Med* 8, 335-352.

[20] Voest, E.E., Kenyon, B.M., O'Reilly, M.S., Truitt, G., D'Amato, R.J., Folkman, J. (1995), Inhibition of angiogenesis in vivo by interleukin 12. *J Natl Cancer Inst* 87, 581-6.

[21] Morini, M., Albini, A., Lorusso, G., Moelling, K., Lu, B., Cilli, M., *et al.* (2004), Prevention of angiogenesis by naked DNA IL-12 gene transfer: angioprevention by immunogene therapy. *Gene Ther* 11, 284-91.

[22] Chen, Z., Varney, M.L., Backora, M.W., Cowan, K., Solheim, J.C., Talmadge, J.E., *et al.* (2005), Down-regulation of vascular endothelial cell growth factor-C expression using small interfering RNA vectors in mammary tumors inhibits tumor lymphangiogenesis and spontaneous metastasis and enhances survival. *Cancer Res* 65, 9004-11.

[23] Morimoto, J., Imai, S., Haga, S., Iwai, Y., Iwai, M., Hiroishi, S., *et al.* (1991), New murine mammary tumor cell lines. *In vitro Cell Dev Biol* 27A, 349-351.

[24] Shibata, M.A., Morimoto, J., Otsuki, Y. (2002), Suppression of murine mammary carcinoma growth and metastasis by HSV*tk*/GCV gene therapy using *in vivo* electroporation. *Cancer Gene Ther* 9, 16-27.

[25] Shibata, M.A., Ito, Y., Morimoto, J., Otsuki, Y. (2004), Lovastatin inhibits tumor growth and lung metastasis in mouse mammary carcinoma model: a p53-independent mitochondrial-mediated apoptotic mechanism. *Carcinogenesis* 25, 1887-1898.

[26] Czauderna, F., Santel, A., Hinz, M., Fechtner, M., Durieux, B., Fisch, G., *et al.* (2003), Inducible shRNA expression for application in a prostate cancer mouse model. *Nucleic Acids Res* 31, e127.

[27] Shibata, M.A., Morimoto, J., Doi, H., Morishima, S., Naka, M., Otsuki, Y. (2007), Electrogene therapy using endostatin, with or without suicide gene therapy, suppresses murine mammary tumor growth and metastasis. *Cancer Gene Ther* 14, 268-278.

[28] Shibata, M.A., Liu, M.-L., Knudson, M.C., Shibata, E., Yoshidome, K., Bandy, T., *et al.* (1999), Haploid loss of *bax* leads to accelerated mammary tumor development in C3(1)/SV40-TAg transgenic mice: reduction in protective apoptotic response at the preneoplastic stage. *EMBO J* 18, 2692-2701.

[29] Gorrin-Rivas, M.J., Arii, S., Furutani, M., Mizumoto, M., Mori, A., Hanaki, K., *et al.* (2000), Mouse macrophage metalloelastase gene transfer into a murine melanoma suppresses primary tumor growth by halting angiogenesis. *Clin Cancer Res* 6, 1647-1654.

[30] Sleeman, J.P. (2000), The lymph node as a bridgehead in the metastatic dissemination of tumors. *Recent Results Cancer Res* 157, 55-81.

[31] Valtola, R., Salven, P., Heikkila, P., Taipale, J., Joensuu, H., Rehn, M., *et al.* (1999), VEGFR-3 and its ligand VEGF-C are associated with angiogenesis in breast cancer. *Am J Pathol* 154, 1381-90.

[32] Achen, M.G., Mann, G.B., Stacker, S.A. (2006), Targeting lymphangiogenesis to prevent tumour metastasis. *Br J Cancer* 94, 1355-60.

[33] Albuquerque, R.J., Hayashi, T., Cho, W.G., Kleinman, M.E., Dridi, S., Takeda, A., *et al.* (2009), Alternatively spliced vascular endothelial growth factor receptor-2 is an essential endogenous inhibitor of lymphatic vessel growth. *Nat Med* 15, 1023-30.

[34] Shibata, M.A., Ambati, J., Shibata, E., Albuquerque, R.J., Morimoto, J., Ito, Y., *et al.* (2010), The endogenous soluble VEGF receptor-2 isoform suppresses lymph node metastasis in a mouse immunocompetent mammary cancer model. *BMC Med* 8, 69.

[35] Kaipainen, A., Korhonen, J., Mustonen, T., van Hinsbergh, V.W., Fang, G.H., Dumont, D., *et al.* (1995), Expression of the fms-like tyrosine kinase 4 gene becomes restricted to lymphatic endothelium during development. *Proc Natl Acad Sci U S A* 92, 3566-70.

[36] Joukov, V., Pajusola, K., Kaipainen, A., Chilov, D., Lahtinen, I., Kukk, E., *et al.* (1996), A novel vascular endothelial growth factor, VEGF-C, is a ligand for the Flt4 (VEGFR-3) and KDR (VEGFR-2) receptor tyrosine kinases. *EMBO J* 15, 290-98.

[37] Shimizu, K., Kubo, H., Yamaguchi, K., Kawashima, K., Ueda, Y., Matsuo, K., *et al.* (2004), Suppression of VEGFR-3 signaling inhibits lymph node metastasis in gastric cancer. *Cancer Sci* 95, 328-33.

[38] Lin, J., Lalani, A.S., Harding, T.C., Gonzalez, M., Wu, W.W., Luan, B., *et al.* (2005), Inhibition of lymphogenous metastasis using adeno-associated virus-mediated gene transfer of a soluble VEGFR-3 decoy receptor. *Cancer Res* 65, 6901-9.

[39] Cao, Y., Linden, P., Farnebo, J., Cao, R., Eriksson, A., Kumar, V., *et al.* (1998), Vascular endothelial growth factor C induces angiogenesis in vivo. *Proc Natl Acad Sci U S A* 95, 14389-94.

[40] McColl, B.K., Stacker, S.A., Achen, M.G. (2004), Molecular regulation of the VEGF family -- inducers of angiogenesis and lymphangiogenesis. *APMIS* 112, 463-80.

[41] Angiolillo, A.L., Sgadari, C., Taub, D.D., Liao, F., Farber, J.M., Maheshwari, S., *et al.* (1995), Human interferon-inducible protein 10 is a potent inhibitor of angiogenesis in vivo. *J Exp Med* 182, 155-62.

[42] Robertson, M.J., Cameron, C., Atkins, M.B., Gordon, M.S., Lotze, M.T., Sherman, M.L., *et al.* (1999), Immunological effects of interleukin 12 administered by bolus intravenous injection to patients with cancer. *Clin Cancer Res* 5, 9-16.

[43] Leonard, J.P., Sherman, M.L., Fisher, G.L., Buchanan, L.J., Larsen, G., Atkins, M.B., *et al.* (1997), Effects of single-dose interleukin-12 exposure on interleukin-12-associated toxicity and interferon-gamma production. *Blood* 90, 2541-8.

[44] Cohen, J. (1995), IL-12 deaths: explanation and a puzzle. *Science* 270, 908.

[45] Mazzolini, G., Narvaiza, I., Martinez-Cruz, L.A., Arina, A., Barajas, M., Galofre, J.C., *et al.* (2003), Pancreatic cancer escape variants that evade immunogene therapy through loss of sensitivity to IFNgamma-induced apoptosis. *Gene Ther* 10, 1067-78.

[46] Nakamori, M., Iwahashi, M., Nakamura, M., Ueda, K., Zhang, X., Yamaue, H. (2003), Intensification of antitumor effect by T helper 1-dominant adoptive immunogene therapy for advanced orthotopic colon cancer. *Clin Cancer Res* 9, 2357-65.

[47] Yamazaki, M., Straus, F.H., Messina, M., Robinson, B.G., Takeda, T., Hashizume, K., *et al.* (2004), Adenovirus-mediated tumor-specific combined gene therapy using Herpes simplex virus thymidine/ganciclovir system and murine interleukin-12 induces effective antitumor activity against medullary thyroid carcinoma. *Cancer Gene Ther* 11, 8-15.

[48] Bloquel, C., Fabre, E., Bureau, M., Scherman, D. (2004), Plasmid DNA electrotransfer for intracellular and secreted proteins expression: new methodological developments and applications. *J Gene Med* 6, S11-S23.

[49] Carter, C.L., Allen, C., Henson, D.E. (1989), Relation of tumor size, lymph node status, and survival in 24,740 breast cancer cases. *Cancer* 63, 181-187.

SAGE-Hindawi Access to Research
International Journal of Breast Cancer
Volume 2011, Article ID 867152, 10 pages
doi:10.4061/2011/867152

Research Article

Lymphangiogenesis and Axillary Lymph Node Metastases Correlated with VEGF-C Expression in Two Immunocompetent Mouse Mammary Carcinoma Models

Yuko Ito,[1] Masa-Aki Shibata,[2] Nabil Eid,[1] Junji Morimoto,[3] and Yoshinori Otsuki[1]

[1] *Division of Life Sciences, Department of Anatomy and Cell Biology, Osaka Medical College, 2-7 Daigaku-Machi, Takatsuki, Osaka 569-8686, Japan*
[2] *Laboratory of Anatomy and Histopathology, Faculty of Health Science, Osaka Health Science University, 1-9-27 Temma, Kita-ku, Osaka 530-0043, Japan*
[3] *Laboratory Animal Center, Osaka Medical College, 2-7 Daigaku-Machi, Takatsuki, Osaka 569-8686, Japan*

Correspondence should be addressed to Yuko Ito, an1006@art.osaka-med.ac.jp

Received 15 June 2011; Accepted 17 August 2011

Academic Editor: Luciane R. Cavalli

Lymphangiogenesis and the expression of vascular endothelial cell growth factor C (VEGF-C) in tumors have been considered to be causally promoting lymphatic metastasis. There are only a few studies on lymphatic metastasis in immunocompetent allograft mouse models. To study the relationship between VEGF-C-mediated lymphangiogenesis and axillary lymph node metastasis, we used two mouse mammary carcinoma cell lines; the BJMC338 has a low metastatic propensity, whereas the BJMC3879 has a high metastatic propensity although it originated from the former cell line. Each cell line was injected separately into two groups of female BALB/*c* mice creating *in vivo* mammary cancer models. The expression level of VEGF-C in BJMC3879 was higher than BJMC338. As the parent cell line, BJMC3879-derived tumors showed higher expression of VEGF-C compared to BJMC338-derived tumors. This higher expression of VEGF-C in BJMC3879-derived tumors was associated with marked increase in infiltrating macrophages and enhanced expression of lymphatic vessel endothelial hyaluronan receptor-1 (LYVE-1) reflecting increased tumoral lymphatic density and subsequent induction of axillary lymph node metastasis. Our mouse mammary carcinoma models are allotransplanted tumors showing the same axillary lymph node metastatic spectrum as human breast cancers. Therefore, our mouse models are ideal for exploring the various molecular mechanisms of cancer metastasis.

1. Introduction

Based on clinical and pathological observations in human mammary carcinomas, the metastatic spread of mammary carcinoma cells is responsible for the majority of cancer deaths [1–5]. The common pathway of initial cancer dissemination is via lymphatics due to their characteristic endothelial structure with blind-ending capillaries [6]. In addition, metastasis to the regional lymph nodes through the lymphatic vessels is considered to be a common step in the progression of cancer and an important prognostic factor in many types of cancer including breast carcinomas. Lymphatic vessel density (LVD) in many types of solid cancer is associated with lymph node metastasis or poor prognosis, as has been reported in experimental and clinical studies [1–5, 7, 8]. Although mammary carcinoma is well known to have the character for lymph node metastasis, there are only a few mouse mammary carcinoma models showing extensive metastasis to lymph nodes. The chick embryo chorioallantoic membrane [9] and immunodeficient mice, SCID mice, or nude mice were used as xenotransplanted host animals to examine metastasis [10–12]. Recent studies have shown the important roles of tumor-associated macrophages (TAMs) expressing CD68 in cancer-mediated lymphangiogenesis [13–15]. Accordingly, the mouse immunocompetent model appears to be necessary for studying lymphangiogenesis and lymph node metastasis.

The vascular endothelial growth factor C (VEGF-C) is a major lymphangiogenic factor. There is some evidence that VEGF-C promotes lymphangiogenesis under several

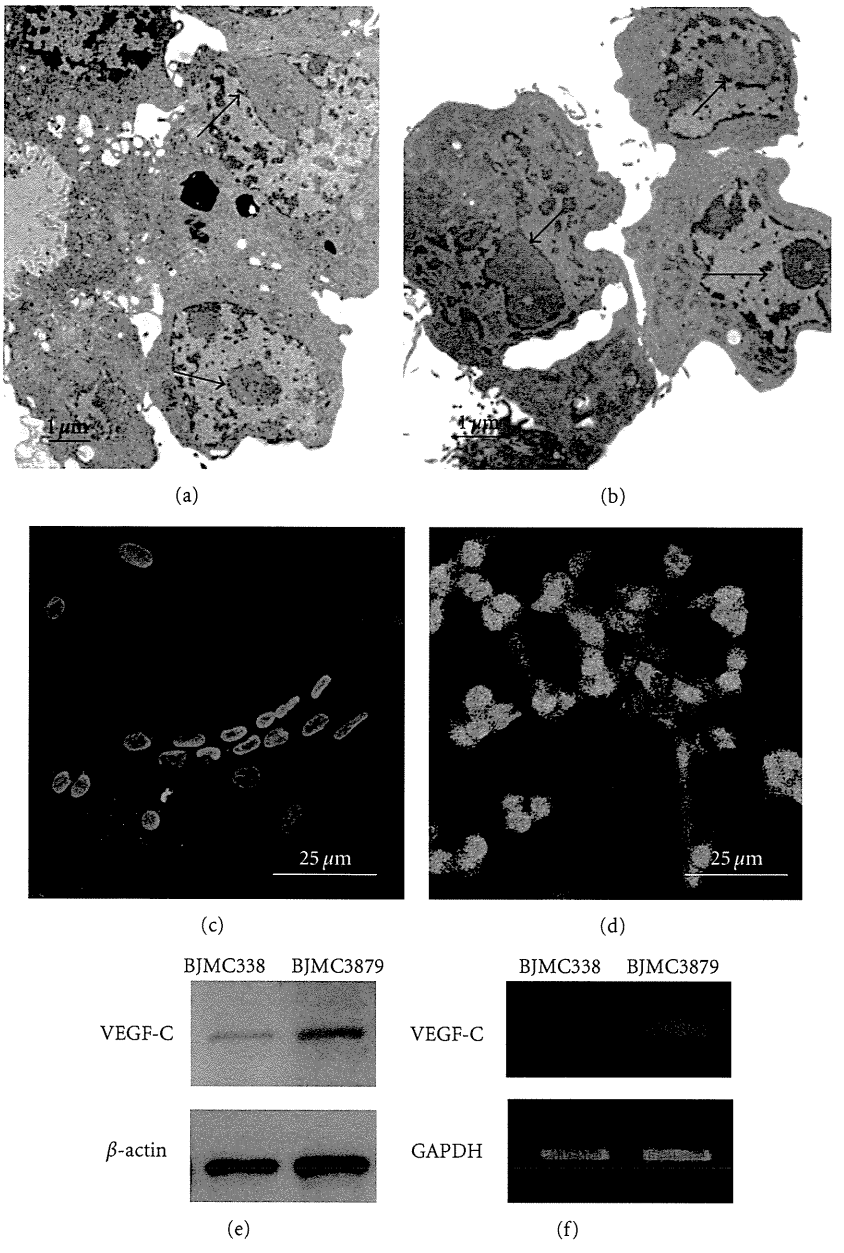

FIGURE 1: TEM micrographs (a and b), immunofluorecent staining (c and d), Western blot analysis (e), and RT-PCR analysis (f) of VEGF-C in the two-mouse mammary carcinoma cell lines. Both BJMC338 cells (a) and BJMC3879 cells (b) have the similar ultrastructure. BJMC338 cells (c) have minimally any activity of VEGF-C, whereas BJMC3879 cells (d) have moderate expression. Western blot analysis (e) demonstrates the same activity of VEGF-C as in (c and d). VEGF-C mRNA expression in BJMC3879 cells is higher than that of BJMC338 cells (f). Green fluorescence (FITC) indicates activity of VEGF-C, and red fluorescence (PI) shows nuclei of cells in (c and d).

normal and pathological conditions [16]. In VEGF-C-deficient mouse embryos, lymphatic vessels fail to develop from veins [17] resulting in prenatal death owing to fluid accumulation in the tissues of mouse embryos and edema in adults [18]. On the other hand, in VEGF-C transgenic mice, hyperplasia of lymphatic vasculature has been reported [19, 20].

To study the relationship between lymphangiogenesis mediated by VEGF-C and axillary lymph node metastasis, two-mouse mammary carcinoma cell lines with different metastatic properties were used in this study. Both cell lines were derived from the same BALB/*c* mouse, one of them, the BJMC338 cell line, an adenocarcinoma cell line, has a low metastatic propensity, whereas the other cell line, BJMC3879, has a high metastatic propensity, particularly to lymph nodes and lungs [21]. Each cell line was injected separately into two groups of adult female BALB/*c* mice creating *in vivo* mammary cancer models. In this inoculation study, we found that increased expression of tumor-derived VEGF-C correlates with LVD and axillary lymph node metastasis.

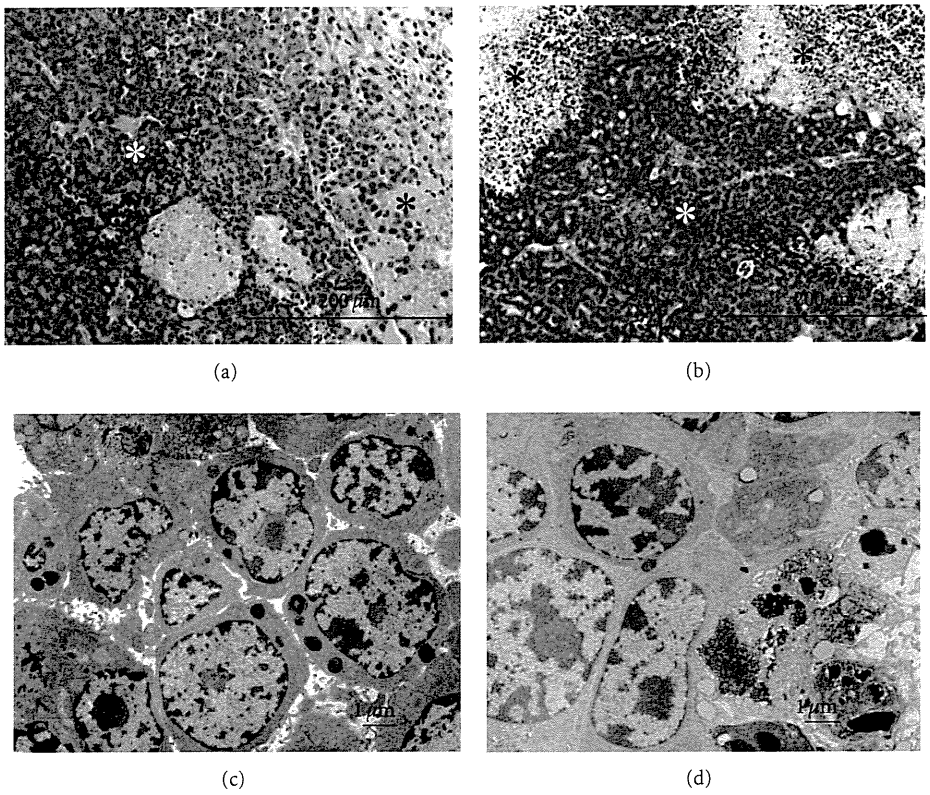

FIGURE 2: Histopathology of the inoculated tumors at 10 weeks postinoculation. H&E staining (a and b) show viable region (white $*$) and necrotic region (black $*$) in BJMC338 tumor (a) and BJMC3879 tumor (b). TEM micrographs (c and d) indicate tumor cells in the viable region of BJMC338 tumor (c) and BJMC3879 tumor (d).

2. Materials and Methods

2.1. In Vitro Studies

2.1.1. Cell Culture and Cell Preparation. Two-mouse mammary carcinoma cell lines were used in this study. The BJMC338 mammary adenocarcinoma cell line used in this study was derived from a female BALB/*c* mouse infected with mouse mammary tumor virus (MMTV) into the inguinal mammary glands and shows low metastatic property. The BJMC3879 mammary adenocarcinoma cell line was derived from foci within metastatic lymph node and lung of a female BALB/*c* mouse that had been injected with BJMC338 cell line into the right inguinal region. The BJMC3879 mammary cell line shows a high metastatic propensity, especially to lymph nodes and lungs [22]. Both cell lines were maintained in RPMI 1640 medium containing 10% fetal bovine serum (FBS) with streptomycin/penicillin in an incubator under 5% CO_2. The cells were immediately rinsed with 0.01 M phosphate buffered saline (PBS), fixed with 2% paraformaldehyde and 2.5% glutaraldehyde in 0.1 M phosphate buffer (PB) (pH 7.4) for 1 h, for transmission electron microscopy (TEM). Cells were subsequently postfixed in 1% OsO_4 for 45 min at room temperature, dehydrated in a series of graded ethanol concentrations, cleared in propylene oxide, and embedded in an epoxy resin mixture. For immunofluorescent study, cells were fixed with 1% paraformaldehyde in PBS for 10 min.

TABLE 1: Number of mice which have lung and axially lymphnode metastases. Metastases were confirmed by H&E staining.

Lung	4W	6W	8W	10W
BJMC338	0	0	0	0
BJMC3879	0	0	5	5
Axially lymph node	4W	6W	8W	10W
BJMC338	0	0	0	0
BJMC3879	0	5	5	5

2.1.2. TEM. After preparation, ultrathin sections were prepared and stained with uranyl acetate and lead citrate. Sixty nm sections were examined by TEM using H-7100 and H-7650 (Hitachi, Tokyo, Japan).

2.1.3. Immunofluorescent Study. Following fixation, cells were transferred to PBS for 15 min, followed by exposure to 1% Block Ace (Dainippon Sumitomo Pharma Co., Ltd., Tokyo, Japan) for 20 min to block nonspecific antibody binding. Cells were then incubated with a primary rabbit anti-VEGF-C antibody (rabbit polyclonal; Santa Cruz Biotechnology, Santa Cruz, Calif, USA) for 1 h at room temperature (RT). After rinse in PBS for 15 min, cells were incubated with a secondary fluorescein-isothiocyanate- (FITC-) conjugated anti-rabbit antibody (Dako, Carpenteria, Calif, USA) for

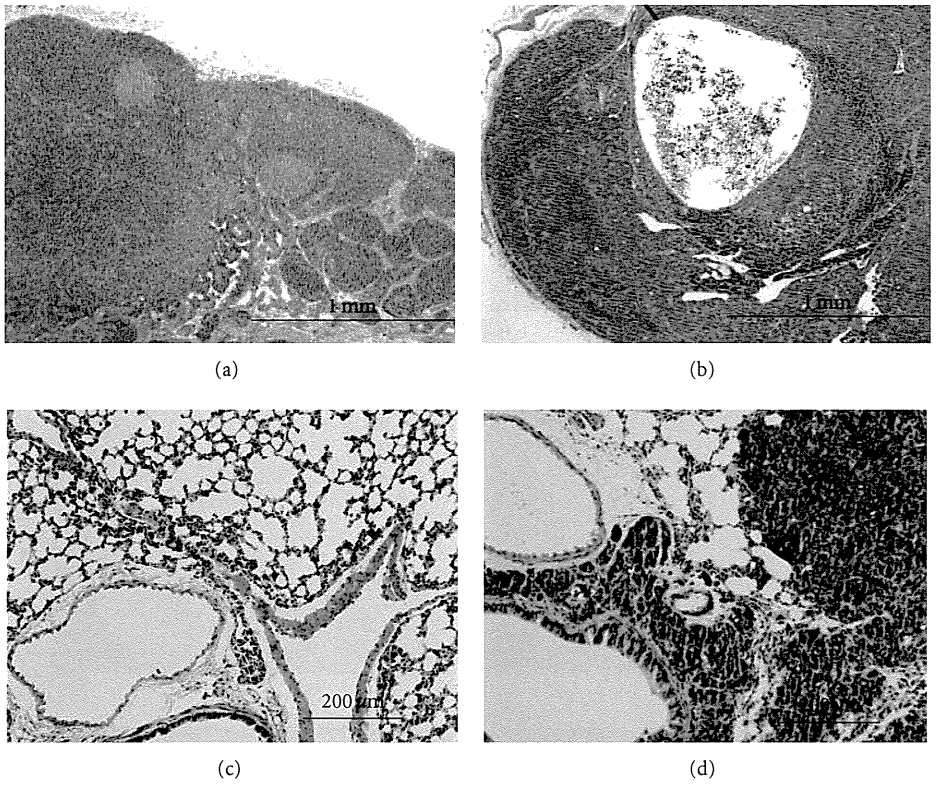

FIGURE 3: Histopathology by H&E staining of axially lymph nodes (a and b) and lungs (c and d) in mice at 10 weeks postinoculation. Axially lymph node and lung in BJMC338 tumor (a and c) show normal appearance, whereas those of BJMC3879 tumor (b and d) demonstrate metastatic foci.

30 min at RT. Samples were counterstained with propidium iodide (PI) for 15 min and observed under a model Radiance 2000 MP confocal scanning laser microscopy (Bio-Rad, Hercules, Calif, USA).

2.1.4. Western Blot Analysis for VEGF-C Protein. Samples containing 20 μg of protein from cultured cells and tumors were fractionated in 10% Tris-glycine gels under reducing conditions and transferred onto nitrocellulose membrane. Anti-VEGF-C antibody (Santa Cruz Biotechnology) was applied to membranes, incubated with appropriate horseradish peroxidase-conjugated secondary antibody, and visualized on X-ray films using enhanced chemiluminescence (Perkin Elmer Life Science, Inc., Boston, Mass, USA).

2.1.5. RNA Preparation and Reverse Transcription-Polymerase Chain Reaction (RT-PCR). Total RNA was isolated from cultured BJMC338 and BJMC3879 cells using an RNeasy Mini Kit (Qiagen, Hilden, Germany) and cDNA Synthesis Kit (Roche Diagnostic Kit, Hilden, Germany) following the manufacturer's protocol, with the total mRNA concentration adjusted to 5 μg/μL in each sample. Primer sequences for VEGF-C were 5′-CCTTCTTTAAACCTCCATGTGT-3′ and 5′-GCAAAACTGATTGTGACTGGT-3′; for glyceraldehyde-3-phosphate dehydrogenase (GAPDH) used as internal control 5′-TGCACGGGAAGCTCACTGG-3′, 5′-TCCACCACCCTGTTGCTGTA-3′ (Nihon Gene Research Laboratories, Sendai, Japan). Products were amplified in a GeneAmp PCR System 9700 (Applied Biosystems, Foster City, Calif, USA) with preincubation at 98°C for 3 min followed by 30 cycles of 94°C for 30 s, 58°C for 30 s, and 72°C for 60 s. The amplification was finished with a single-3 min incubation at 72°C. The PCR products were separated on 1.5% agarose gels, stained with 0.1 mg/mL ethidium bromide, visualized by UV transillumination, and documented on black and white instant films.

2.2. In Vivo Studies

2.2.1. Animals and Preparation of Tumors. A total of 40 female 6-week-old BALB/*c* mice (Japan SLC Inc., Hamamatsu, Japan) were used in this study. All manipulations of mice were performed in accordance with the procedures outlined in the Guide for Care and Use of Laboratory Animals in Osaka Medical College. Mice were divided into two groups (20 mice each), and BJMC338 and BJMC3879 cells (5×10^6 cells/0.3 mL in PBS) were inoculated subcutaneously into right inguinal region, respectively. Mice were sacrificed at 4, 6, 8, 10 weeks after inoculation under ether anesthesia. Tumor samples were frozen for Western blot assay and RT-PCR. Another one was fixed for histopathology and immunohistochemistry with 4 or 10% paraformaldehyde, and for electron microscopy in a same fixative as *in vitro* study. Lungs and right axillary lymph nodes of mice were

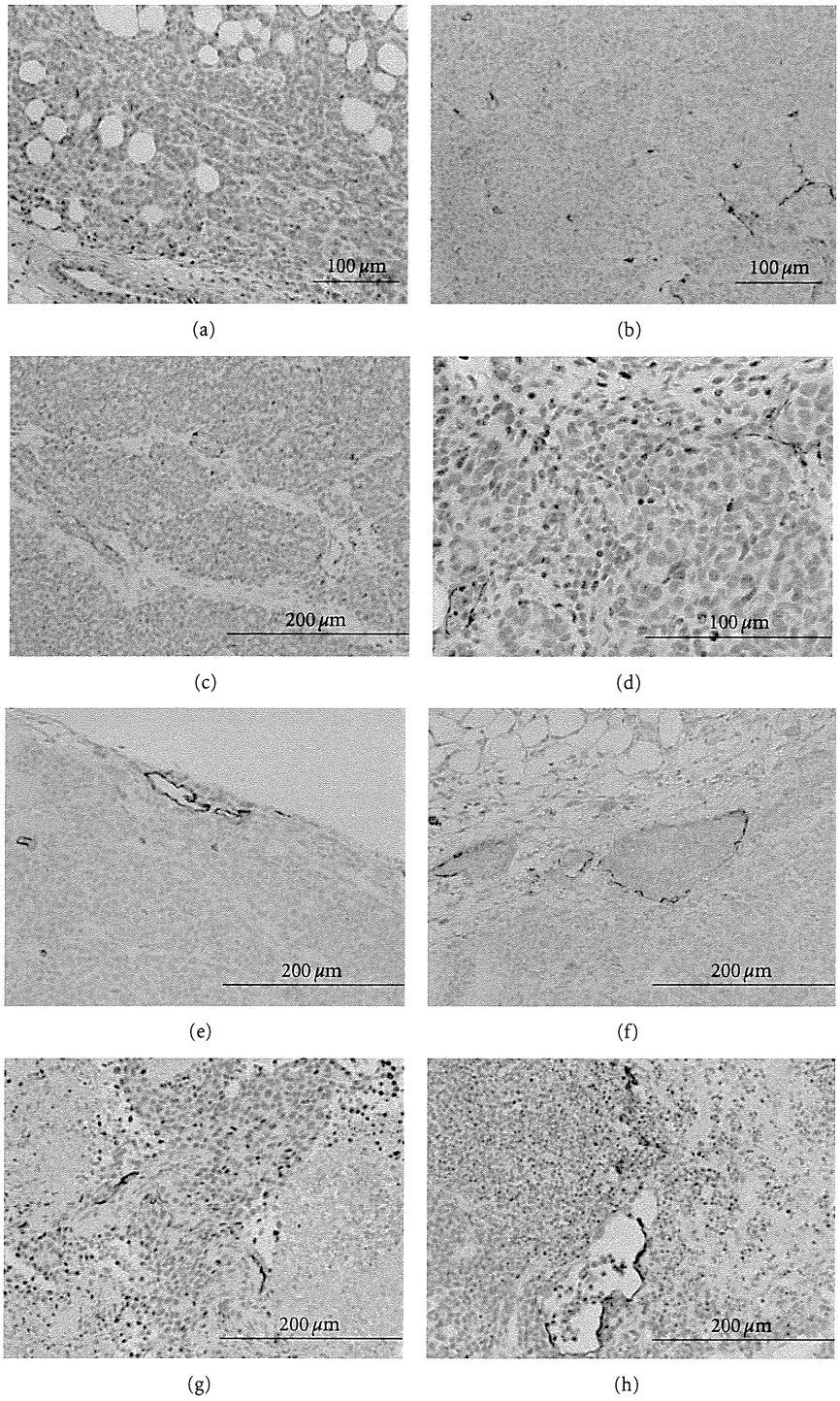

FIGURE 4: Immunohistochemistry of LYVE-1 in BJMC338 tumors (a, c, e, and g) and BJMC3879 tumors (b, d, f, and h) at 4 weeks (a and b), 6 weeks (c and d), 8 weeks (e and f), and 10 weeks postinoculation (g and h). Note the upregulation of LYVE-1 in BJMC3879 tumors.

removed and then fixed as same as tumors. Samples fixed with paraformaldehyde were processed through to paraffin embedding.

2.2.2. Histopathology and Immunohistochemistry. To examine histopathology and metastasis, tumors, lungs, and light axillary lymph nodes were stained with Hematoxylin and Eosin (H&E). Ultrastructural features of tumors were checked under TEM. The avidin-biotin complex method was used for immunohistochemistry. To visualize lymphatic vessels, tumors were stained with primary antibodies to the lymphatic-specific marker, lymphatic vessel endothelial

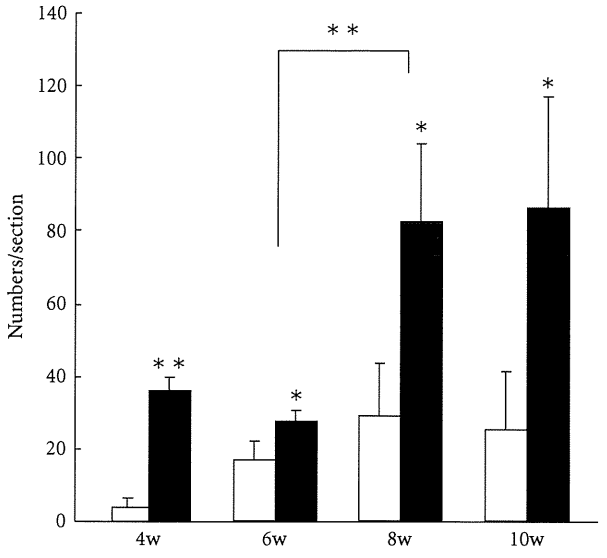

FIGURE 5: Density of lymphatic vessels (LVD) in tumors. The LVD in BJMC3879 tumors (black bars) is always significantly higher than that of BJMC338 tumors (white bars) ($*P < 0.01$, $**P < 0.001$).

hyaluronan receptor-1 (LYVE-1) (rabbit polyclonal, Acris Antibodies GmbH, Hiddenhausen, Germany). VEGF-C (Santa Cruz) was labeled on tumor sections, and activated macrophages were demonstrated by CD68 antibody (rat anti-mouse CD68, AbD Serotec, Oxford, UK).

2.2.3. Lymphatic Vessel Density (LVD) and Counting of Macrophage. The number of lymphatic vessels immunolabeled with anti-LYVE-1 antibody in tumor sections at 4 to 10 weeks postinoculation as well as the number of CD68-positive cells in tumor sections at 4 weeks postinoculation were counted under light microscopy at higher magnification (×200).

2.2.4. Statistical Analysis. The above-mentioned data were analyzed by Student's t-test. $P < 0.05$ was considered statistically significant.

3. Results

3.1. In Vitro Studies

3.1.1. Ultrastructure and Expression of VEGF-C. Ultrastructural differences between BJMC338 and BJMC3879 cells were investigated using TEM. Both cell lines showed the same morphology under TEM (Figures 1(a) and 1(b)). They had prominent nucleoli and dispersed small condensed chromatin in their nuclei. By immunofluorescent study, VEGF-C was barely expressed in BJMC338 cells, whereas moderately expressed in BJMC3879 cells (Figures 1(c) and 1(d)). The levels of VEGF-C protein in the two cell lines were determined by Western blot; the intensity of the bands was measured and corrected against β-actin intensity. A moderate increase in the VEGF-C protein level was detected in BJMC3879 cells (Figure 1(e)). RT-PCR analysis showed higher VEGF-C mRNA expression in BJMC3879 cells than in BJMC338 cells (Figure 1(f)).

3.2. In Vivo Studies

3.2.1. Histopathology and Metastasis. Histopathologically, the two types of inoculated mammary carcinoma (BJMC338 and BJMC3879 tumors) proved to be moderately differentiated adenocarcinomas. Both tumors were accompanied by a viable region, a central necrosis, and an inflammatory region (Figures 2(a) and 2(b)). The morphology of the tumor cells in the viable region was the same as that of the cultured cell lines (Figures 2(c) and 2(d)). Metastasis to axillary lymph nodes or lungs at 8 and 10 weeks postinoculation was validated by the observation of sections stained with H&E. At 8 and 10 weeks postinoculation, no metastasis was observed in the lymph nodes and lungs of mice that were inoculated with BJMC338 cells (Figures 3(a) and 3(c)). In contrast, all the mice inoculated with BJMC3879 cells showed distant metastasis to axillary lymph nodes and lungs at 8 and 10 weeks postinoculation (Table 1, Figures 3(b) and 3(d)).

3.2.2. Lymphangiogenesis in Tumor Mouse Models. The lymphatic vessels in the tumor were detected by immunohistochemistry using the antibody specific to lymphatic vessels, LYVE-1. At 4 weeks postinoculation, few lymphatic vessels were found in BJMC338 tumors (Figure 4(a)). At 6 weeks postinoculation, several lymphatic vessels were observed in intratumoral connective tissues and/or surrounding connective tissues (Figures 4(c), 4(e), and 4(g)). Conversely, large numbers of dilated lymphatic vessels with or without tumor cells were observed within and around BJMC3879 tumors at 4 to 10 weeks postinoculation (Figures 4(b), 4(d), 4(f), and 4(h)).

3.2.3. Lymphatic Vessel Density (LVD). The LVD of BJMC3879 tumors was always significantly higher than that of BJMC338 tumors (Figure 5). In BJMC338 tumors, the LVD at 6 weeks postinoculation was significantly higher than that at 4 weeks postinoculation ($P < 0.01$), after that, no significant difference in the LVD was observed (Figure 5). However, in BJMC3879 tumors, the difference in the LVD between 8 and 10 weeks postinoculation was not significant; a significant difference was detected between 6 and 8 weeks postinoculation ($P < 0.001$), namely, the LVD markedly increased at 8 weeks postinoculation (Figure 5).

3.2.4. TEM for Lymphatic Vessels. The status and ultrastructural features of lymphatic vessels in inoculated tumors were examined under TEM. Lymphatic capillaries were observed in the connective tissue surrounding and inside the tumors. They were distinguished from blood capillaries. The examination of lymphatic capillaries revealed that they had thin endothelium, abluminal protrusion of endothelial cells, no pericyte, no lamina densa, and overlapping junctions (Figures 6(a)–6(d)). Intraluminal tumor cells were observed in their lumen (Figure 6(a)). Interestingly, a leukocyte was shown to go into and/or out from the

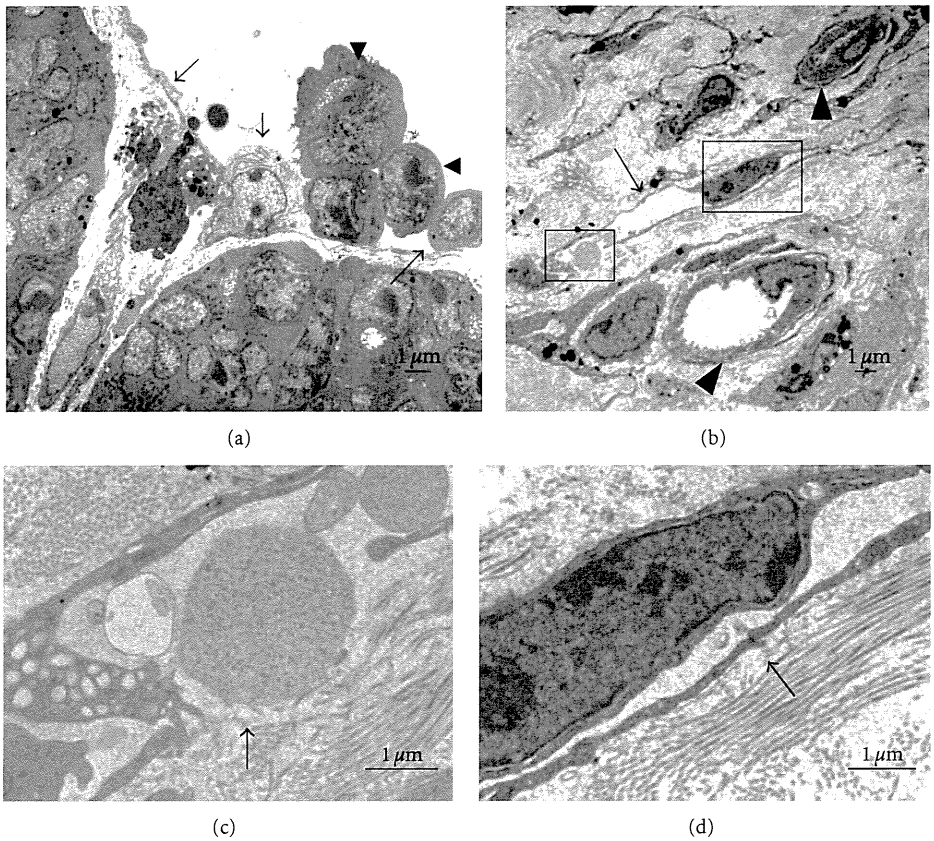

FIGURE 6: TEM micrographs of lymphatic vessels in BJMC3879 tumors at 10 weeks postinoculation (a) and 4 weeks postinoculation (b). The boxed areas in (b) are observed with high-power view (c and d). (a) A leukocyte (∗) is seen between endothelial cells (arrows), whereas tumor cells (arrowheads) are observed in the lumen. (b) Lymphatic capillary (arrow) and blood capillaries (arrowheads) are detected in the connective tissue surrounding tumors. Casein-like droplet (arrow) is located in the opening junction (c), and characteristic over-lapping junction (arrow) is showed (d).

lymphatic lumen (Figure 6(a)). Furthermore, the absorption of caseinlike droplets into the lymphatic lumen was observed (Figure 6(c)).

3.2.5. VEGF-C Expression in the Tumors. VEGF-C-positive cells were localized mainly in the peripheral viable regions of tumors. Immunohistochemical studies and Western blot analyses clearly demonstrated weak expression of VEGF-C in BJMC338 tumors (Figures 7(a) and 7(c)), relative to the strong expression in BJMC3879 tumors (Figures 7(b) and 7(c)).

3.2.6. Distribution of CD68-Positive Macrophages in the Tumors. CD68-positive macrophages were found mainly in the viable regions of both tumors (Figure 8). CD68-positve macrophages containing vacuoles in their cytoplasm aggregated in the tumors. The density of macrophages in BJMC3879 tumors was significantly higher than that in BJMC338 tumors ($P < 0.001$) (Figure 8).

4. Discussion

In this study, we found that mouse mammary tumor cells (BJMC3879) that have high metastatic propensity expressed a higher level of VEGF-C than the mouse mammary tumor cells (BJMC338) with low metastatic propensity, and the inoculated BJMC3879 tumors expressed VEGF-C equivalently to tumor cell lines. In highly metastatic mouse mammary tumors (BJMC3879), LVD and the VEGF-C expression level were higher than those in the poorly metastatic mouse mammary tumors (BJMC338). BJMC3879 tumor cell inoculation resulted in axillary lymph node and lung metastases, whereas no metastasis occurred after BJMC338 tumor cell inoculation.

There are some clinical surveys of human breast cancer to prove a causal relationship between LVD and malignancy, the VEGF-C expression, lymph node metastasis, and prognosis [1, 4, 5]. Increased LVD in breast cancer was correlated with lymph node metastasis and VEGF-C expression. It was concluded that a high LVD may be a significant unfavorable prognostic factor for long-term survival of breast cancer patient. Our results correlate with their reports. Contrary to the clinical importance of these LVDs and on the basis of clinicopathological studies including breast cancers, it is the hypothesized that intratumoral lymphatics have no function. None of the breast carcinoma was found to contain Ki-67-positive dividing endothelial cells of lymph vessels [23], and by experimental microlymphangiography assay, no